

**\*\*FULL TITLE\*\***

*ASP Conference Series, Vol. \*\*VOLUME\*\*, \*\*YEAR OF PUBLICATION\*\**

**\*\*NAMES OF EDITORS\*\***

## Physical conditions in the Homunculus

Gary J. Ferland & Nick Abel

*Physics, University of Kentucky*

Kris Davidson

*Astronomy, University of Minnesota*

Nathan Smith

*CASA, University of Colorado*

**Abstract.** Conditions within the Homunculus nebula around Eta Car are determined by many of the same physical processes that occur in molecular clouds in the interstellar medium. But there is one major exception – we know when the ejection occurred and something about its composition and initial state. The gas was warm, ionized, and dust-free when it was located within the star’s atmosphere and it is currently cold, molecular, and dusty. It undertook this transformation in a bit over 150 years. It offers a laboratory for the study of physical processes in a well-constrained environment. We derive a photoionization model of the Homunculus nebula that reproduces many of its observed properties. We conclude by outlining how observations of the Homunculus could address basic problems in the physics of the interstellar medium.

### 1. Introduction

Eta Carinae, one of the most luminous stars in the Galaxy, offers a laboratory in which a variety of physical phenomena can be studied. The star has undergone at least one episode of substantial mass loss, and is likely to end its life as a supernova. Understanding the physics that occurs within the ejecta will offer insight into the initial stages of chemical enrichment of the interstellar medium. Both molecules and grains are known to have formed in the Homunculus nebula, gas that was ejected in the nineteenth century. The physical conditions in this nebula are the subject of this paper, along with a sketch of how Eta Car might be used as a test bed to understand critical interstellar processes.

### 2. An illustrative model of the Homunculus

The Homunculus nebula is seen in the optical by reflected starlight and is one of the brightest objects in the sky in the mid-IR, showing that substantial amounts of dust are present (Westphal & Neugebauer 1969). In the infrared, emission lines of [Fe II] and H<sub>2</sub> are seen and have been traced across the nebula in long-slit observations (Smith 2002). These show a double-shell structure, with Fe<sup>+</sup>

present in the inner parts of the Homunculus, and  $\text{H}_2$  in the outer zone. Additionally, the Homunculus shows a double-shell structure in the dust color temperature distribution, with a cool outer shell at  $\sim 140$  K and a warmer inner shell at  $\sim 200$ - $250$  K (Smith et al. 2003). These observations help constrain any model of the envelope.

We model the shell as a constant-density layer with an inner radius of  $1.7 \times 10^{17}$  cm and a thickness of  $10^{17}$  cm, appropriate for material in the wall of the southeast polar lobe along our line of sight to the star (Smith 2002; Smith et al. 2003). The electron density in the inner  $\text{Fe}^+$  region, deduced from infrared [Fe II] line ratios, is  $\sim 10^4 \text{ cm}^{-3}$  (Smith 2002). The hydrogen density must be substantially higher here since the gas is mainly neutral. From the geometry of the nebula and the presumed total mass of  $\sim 12 M_\odot$  for the entire Homunculus (Smith et al. 2003), we infer a hydrogen density of  $\sim 10^6 \text{ cm}^{-3}$ . Of course, this depends on the gas-to-dust mass ratio, taken to be 100 (but see below). For these parameters the column density through the shell is  $N_H = 10^{23} \text{ cm}^{-2}$ .

The dust that is clearly present in the nebula will be the catalyst in forming the observed  $\text{H}_2$ . The measured visual extinction is  $A_V \approx 4$  mag, (e.g., Davidson & Humphreys 1997), corresponding to an extinction per unit column density of  $A_V/N_H \approx 4 \times 10^{-23} \text{ mag cm}^2$ . The extinction is observed to be grey and the dust color temperature in the shell is near the equilibrium blackbody temperature (Whitelock et al. 1983; Hillier et al. 2000; Smith et al. 1998, 2003), suggesting that the grains are large. We assume that the grains are similar to those seen in Orion's Veil,  $R=5$ , and assume that only the silicate component is present. This large  $R$  is produced by a grain size distribution that is lacking in small grains, which will affect the  $\text{H}_2$  formation rate and grain photoelectric heating.

The ratio of C/O is less than unity in the ejecta, (Davidson et al. 1986), suggesting that the chemistry will be dominated by oxygen-bearing species once formation of CO is complete, and that the chemistry will eventually lead to oxygen-rich solids, motivating our use of the silicate grain type. The observations of silicate features in the infrared (e.g., Gehrzt et al. 1973), and the absence of a graphite feature in the ultraviolet (Viotti et al. 1989) supports this idea. For simplicity we leave the silicate dust to gas ratio at its ISM value, which corresponds to an extended source  $A_V/N_H \approx 9 \times 10^{-23} \text{ mag cm}^2$ . The grain size distribution and dust to gas ratio will affect the details of our calculations, as well as clumping of the material, but not the overall results.

The assumed gas-phase abundances are listed in Table 1, along with other parameters. Relative to H, He is overabundant, while O is highly underabundant, presumably due to partial CNO cycling. The N/H ratio, roughly ten times solar, corresponds to the conversion of nearly all C and O into N (Davidson et al. 1986; Smith & Morse 2004). Most C is expected to be in the form of the  $^{13}\text{C}$  isotope.

We assume that the stellar continuum is represented by an interpolated 20,000 K CoStar atmosphere with a total luminosity of  $5 \times 10^6 L_\odot$ . We add a high-energy component corresponding to a  $3 \times 10^6$  K blackbody with a luminosity of  $30 L_\odot$  (e.g., Corcoran et al. 2001). The lack of a prominent H II region shows that few hydrogen-ionizing photons strike the inner edge of the nebula, most likely due to photoelectric absorption by the stellar wind. We extinguish the net continuum by photoelectric absorption due to a neutral layer of  $10^{21} \text{ cm}^{-2}$

to account for this. Some high-energy photons are transmitted and they help drive the chemistry. The incident stellar continuum is shown in Figure 1.

We also include the galactic background cosmic ray ionization rate. The actual ionization rate may be higher if radiative nuclei are present. Cosmic rays have effects that are similar to X-rays – they provide ionization that helps drive the chemistry.

### 3. Calculations

We simulate the conditions within the nebula using the development version of Cloudy, last described by Ferland et al. (1998).

Recent updates to Cloudy include an improved molecular network that allow for calculations deep in molecular clouds. Some of these improvements are discussed in Abel et al. (2004). The developmental version of Cloudy currently predicts molecular abundances for  $\sim 70$  molecules involving H, He, C, O, N, Si, and S. Approximately 1000 reactions are in the network, with most reaction rates taken from the latest version of the UMIST database. Our predictions are in good agreement with other codes that are designed to predict conditions in PDRs.

The computed ionization, thermal, and molecular structure are shown in Figures 2 and 3. The emitted continuum is the solid line in Figure 1.

Hydrogen is predominantly atomic at the illuminated face of the cloud. We assume that no H-ionizing radiation escapes from the stellar wind, but the  $H^+$  density at the illuminated face is quite sensitive to the transfer of the incident stellar continuum in the Lyman lines. If it is bright in these lines then hydrogen can become ionized by a two-step process. An excited state is populated by absorption of a Lyman line, which then decays into the  $H^0 2s$  level. The Balmer continuum can photoionize atoms in this state, creating a thin region with  $H^+$  and a high electron density. The Lyman lines quickly become self-shielding and the process is no longer important, although a small amount of  $H^+$  is produced across the nebula by cosmic ray and X-ray ionization.

$H_2$  forms at depth of  $\sim 3.5 \times 10^{16}$  cm, where the Lyman-Werner bands become optically thick, the continuum between  $L\alpha$  and the Lyman limit is heavily extinguished, and the destruction rate of  $H_2$  goes down dramatically. As Figure 1 shows, little light escapes at short wavelengths. Grains are the dominant opacity across the cloud, helping shield  $H_2$  and allowing for efficient formation by catalysis on grain surfaces. The  $Fe^+$  profile is also shown, indicating an anti-correlation between  $Fe^+$  and  $H_2$ . Observations (Smith 2002) show that  $Fe^+$  and  $H_2$  are segregated, occupying the inner and outer zones of the Homunculus walls, respectively, which generally agrees with the structure in Figure 2.

The formation of large amounts of  $H_2$  initiates the formation of heavy-element molecules (see Figure 2 and Table 2).  $H_2$  is a step in the formation of  $H_2^+$  and  $H_3^+$ , the highly reactive ion-molecules that undergo ion-neutral reactions to form molecules containing heavier elements. Large amounts of CO form when its electronic bands become self-shielding. For this calculation, CO fully forms at depth of  $\sim 9 \times 10^{16}$  cm. We assume a C/O abundance ratio of 0.5. At the shielded face the  $n(CO)/n(C_{tot})$  ratio is nearly unity and a significant amount of O is in the form of OH.

Nitrogen is strongly enhanced in the ejecta, and several nitrogen-bearing molecules are shown in Table 2 and Figure 2. As expected,  $N_2$  is the dominant molecule, although only a small amount of N is in this form – N remains predominantly atomic.

The gas temperature is shown in Figure 3. It lies in the range  $\sim 50$  K to  $\sim 300$  K and is typical of a PDR. The temperature is mainly maintained by a balance between grain photoionization heating and cooling by fine structure lines of C, O, Si, and Fe. The temperature falls at the point where  $H_2$  forms due to the strong absorption by its electronic transitions and also by atomic C. In the coldest regions heating by cosmic rays becomes important, together with cooling by CO rotation transitions.

The Homunculus appears “lumpy”, showing that the envelope does not have constant density or pressure. These calculations show two possible sources of local instabilities which might help form blobs. The radiative acceleration, mainly caused by the absorption of the incident continuum by grains and lines, exceeds  $3 \times 10^{-3} \text{ cm s}^{-2}$  at the illuminated face but falls to  $3 \times 10^{-6} \text{ cm s}^{-2}$  at the shielded face. This suggests that significant radiative acceleration can occur over the  $\sim 10^2$  yr lifetime of the ejecta. It may be Rayleigh-Taylor unstable because of the decreasing acceleration. The thermal balance is a second source of instability – the temperature derivative of the net cooling, defined as cooling minus heating, is negative across much of the ejecta; this material is thermally unstable. Both instabilities will be the focus of future work.

The emitted spectrum is shown as the solid line in Figure 1. Thermal infrared emission from grains is prominent, along with CO lines in the mm. The  $10 \mu\text{m}$  silicate feature is present since the calculation only included a silicate component. A detailed comparison with observations would help constrain the model further, and so help deduce properties such as the dust abundance and composition.

#### 4. The Future

Our main purpose is to point to directions for future work on the Homunculus, with the goal of using it as a laboratory to understand basic physical processes. The Homunculus is an especially well-posed problem. The ejecta were once part of a hot stellar atmosphere and so must have initially been warm, ionized, and dust-free. Today it is cold, dusty, and molecular. How did it go between these states during the time since its ejection?

This dust could not have formed in the atmosphere of Eta Car itself, since the energy density temperature is above the condensation temperature of most solids. Thus the dust now seen in reflection is most likely to have formed in the material after being expelled from the star. The cycle of dust destruction and formation is still poorly understood (Draine 1990). These newly formed dust grains have a large size, and measurements of the extinction curve across the spectrum would help quantify their radii. A comparison between intensities of the thermal IR continuum and  $H_2$  or CO lines would measure the dust-to-gas ratio. Infrared spectral features can also reveal the dust composition. This is especially important in light of recent work suggesting that supernovae are important sources of new grains in the galaxy (Morgan et al. 2003).

The Homunculus is predicted to be predominantly molecular. A molecular inventory could be obtained from UV observations of electronic absorption lines or from the many prominent rotational emission lines that are expected in the IR – mm. We have a good idea of the initial gas-phase chemical composition so this inventory would test current chemical reaction networks, and especially the theory of H<sub>2</sub> formation on grain surfaces. The chemistry will be affected by additional cosmic ray ionization if radioactive nuclei are present in the ejecta, and also by the isotopic variations – most C should be <sup>13</sup>C rather than <sup>12</sup>C. Can the chemistry test these assumptions?

Finally, the prominent structures seen in the Homunculus can test dynamical theories. Could thermal or radiation driving instabilities play a role?

Acknowledgments: Research into the physical processes of the ISM is supported by NSF (AST 0307720) and NASA (NAG5-12020). N.S. was supported by NASA through grant HF-01166.01A from STScI, which is operated by AURA, Inc., under NASA contract NAS 5-26555.

## References

- Abel, N.P., Brogan, C.L., Ferland, G.J., O'Dell, C.R., Shaw, G., & Troland, T.H. 2004, *ApJ*, 609, 247
- Corcoran, M.F., et al. 2001, *ApJ*, 547, 1034
- Davidson, K., & Humphreys, R.M. 1997, *ARAA*, 35, 1
- Davidson, K., et al. 1986, *ApJ*, 305, 867
- Draine B. T. 1990, in: *The Evolution of the Interstellar Medium*, ed. L. Blitz, ASP, San Francisco, p. 193
- Ferland, G. J., Korista, K.T., Verner, D.A., Ferguson, J.W., Kingdon J.B., & Verner E.M. 1998, *PASP*, 110, 761
- Gehrz, R.D. et al. 1973, *Astrophys. Lett.*, 13, 89
- Hillier, D.J., et al. 2001, *ApJ*, 553, 837
- Morgan, H.L., Dunne, L., Eales, S.A., Ivison, R.J., & Edmunds, M.G. 2003, *ApJ*, 597L
- Smith, N. 2002, *MNRAS*, 337, 1252
- Smith, N., Gehrz, R.D., & Krautter, J. 1998, *AJ*, 116, 1332
- Smith, N., et al. 2003, *AJ*, 125, 1458
- Smith, N., & Morse, J.A. 2004, *ApJ*, 605, 854
- Viotti, R., et al. 1989, *ApJS*, 71, 983
- Westphal, J.A., & Neugebauer, G. 1969, *ApJ*, 156, L45
- Whitelock, P.A., et al. 1983, *MNRAS*, 203, 385

TABLE 1 – Model parameters

Parameter (Homunculus)	Value	Parameter (Stellar)	
He/H	0.40	Wind extinction	$N_H=10^{21} \text{ cm}^{-2}$
C/H	$4.0 \times 10^{-5}$	Atmosphere	Interp. Costar
N/H	$1.5 \times 10^{-3}$	$T_{eff}$	20,000K
O/H	$7.6 \times 10^{-5}$	$L$	$5 \times 10^6 L_\odot$
Remaining elements	Solar	Corona	
$n_H$	$10^6 \text{ cm}^{-3}$	Atmosphere	blackbody
Inner radius	$1.7 \times 10^{17} \text{ cm}$	$T_{eff}$	$1.3 \times 10^6 \text{ K}$
Thickness	$10^{17} \text{ cm}$	$L$	$30 L_\odot$
Filling factor	1		
Covering factor	0.03		
Grains	R=5 Orion silicate		
Cosmic ray	Galactic Background		

TABLE 2 – Predicted column densities ( $\text{cm}^{-2}$ )

Species	Log $N$	Species	Log $N$	Species	Log $N$
H <sup>0</sup>	22.53	N <sub>2</sub>	14.64	H3 <sup>+</sup>	12.55
H <sub>2</sub>	22.52	CH <sub>2</sub>	13.98	HCO <sup>+</sup>	12.50
N <sup>0</sup>	20.18	CH	13.45	NO	12.48
O <sup>0</sup>	18.86	CH3 <sup>+</sup>	13.27	SiO	12.42
H <sup>+</sup>	18.50	HCS <sup>+</sup>	13.09	HCN	12.41
C <sup>+</sup>	18.27	CS	13.06	HeH <sup>+</sup>	12.23
C <sup>0</sup>	18.24	CN	12.88	SiN	12.21
Fe <sup>0</sup>	18.17	CH <sub>3</sub>	12.87	OH	12.18
Fe <sup>+</sup>	18.13	CH <sub>4</sub>	12.80	NS <sup>+</sup>	12.12
CO	17.54	H <sub>2</sub> O	12.63	CH <sub>5</sub> <sup>+</sup>	12.02

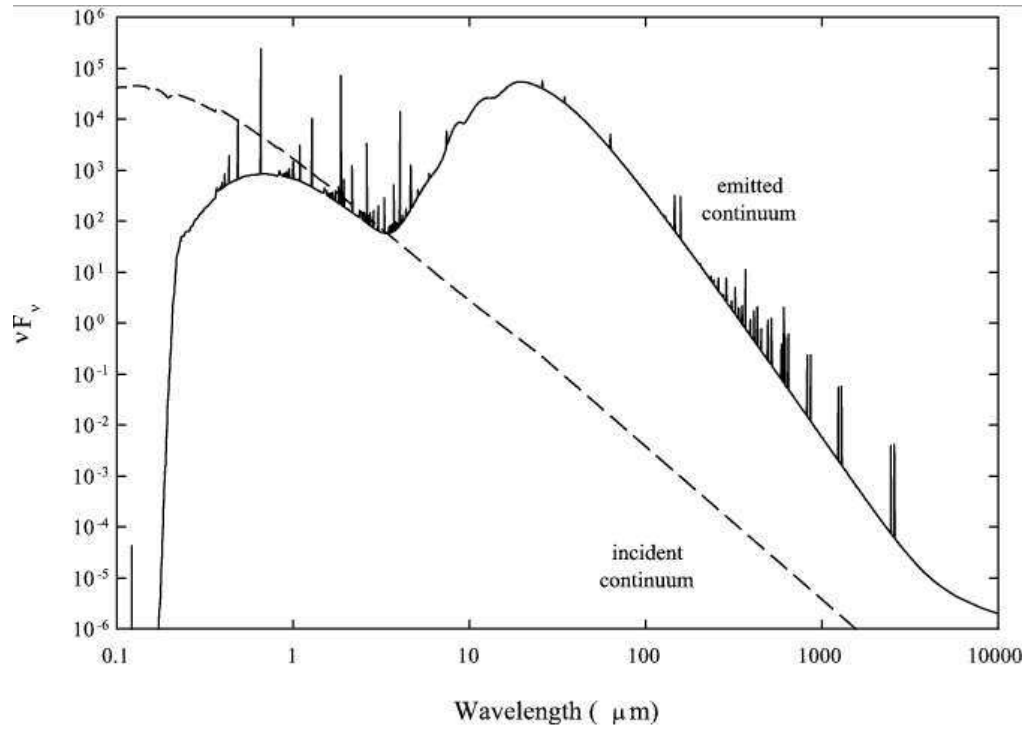


Figure 1. The incident stellar continuum, emitted by the central star, is shown as a dashed line. The predicted emergent continuum is the solid line.

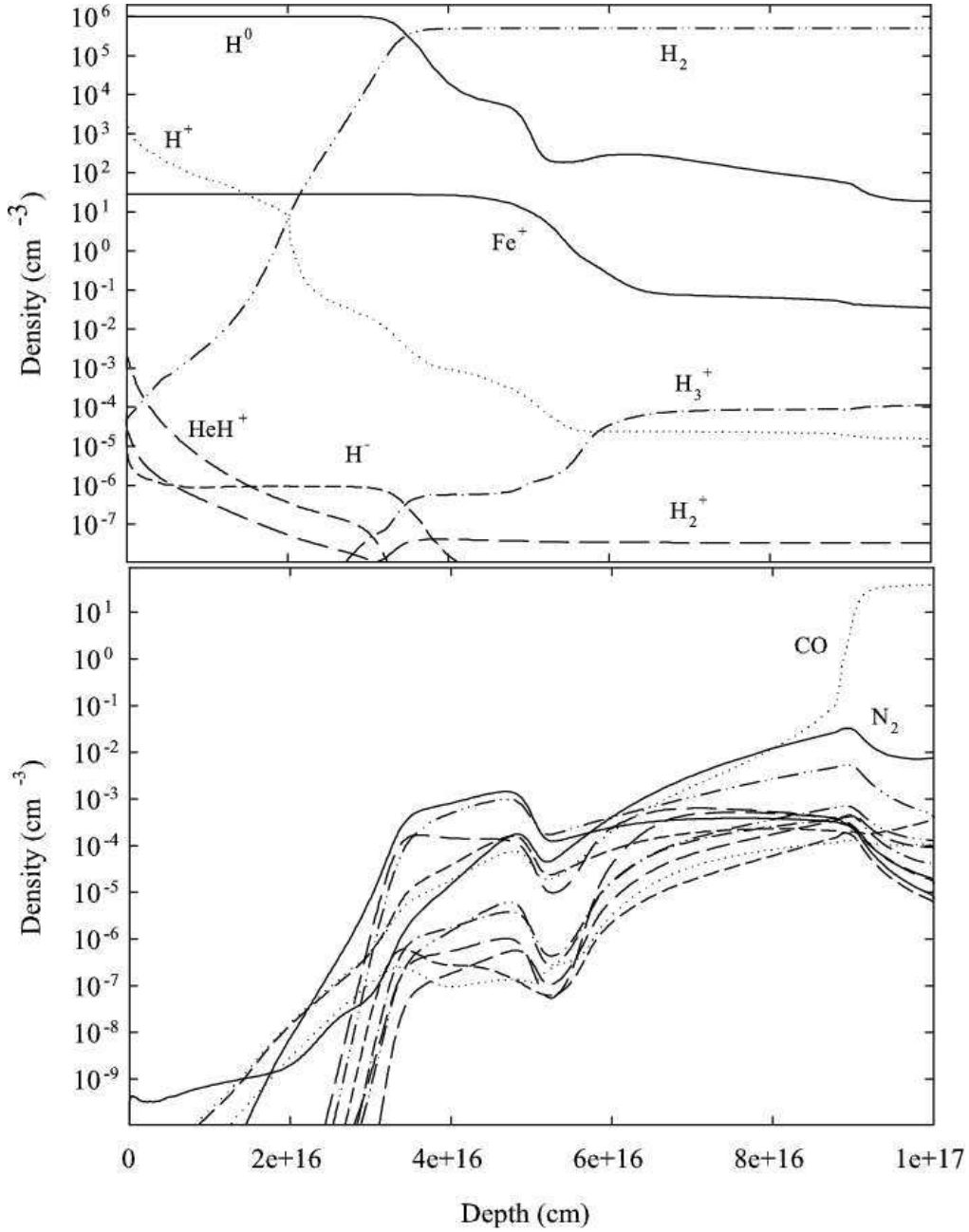


Figure 2. The predicted molecular, atomic, and ionic densities vs depth into the shell. The upper panel shows that the inner half of the shell emits Fe II while  $\text{H}_2$  is found in the outer two-thirds, in agreement with observations. The lower panel gives densities of the major molecular constituents. In the outer-most region CO is the dominant molecule, while  $\text{N}_2$  is the dominant H-carrying species. The text identifies the remaining molecules. At the shielded face the molecules, in order of decreasing abundance, are CO,  $\text{N}_2$ ,  $\text{CH}_2$ ,  $\text{H}_2\text{O}$ , SiO, CS, NO,  $\text{H}_3^+$ ,  $\text{CH}^+$ , SiN,  $\text{HS}^+$ , and  $\text{CH}_5^+$ .



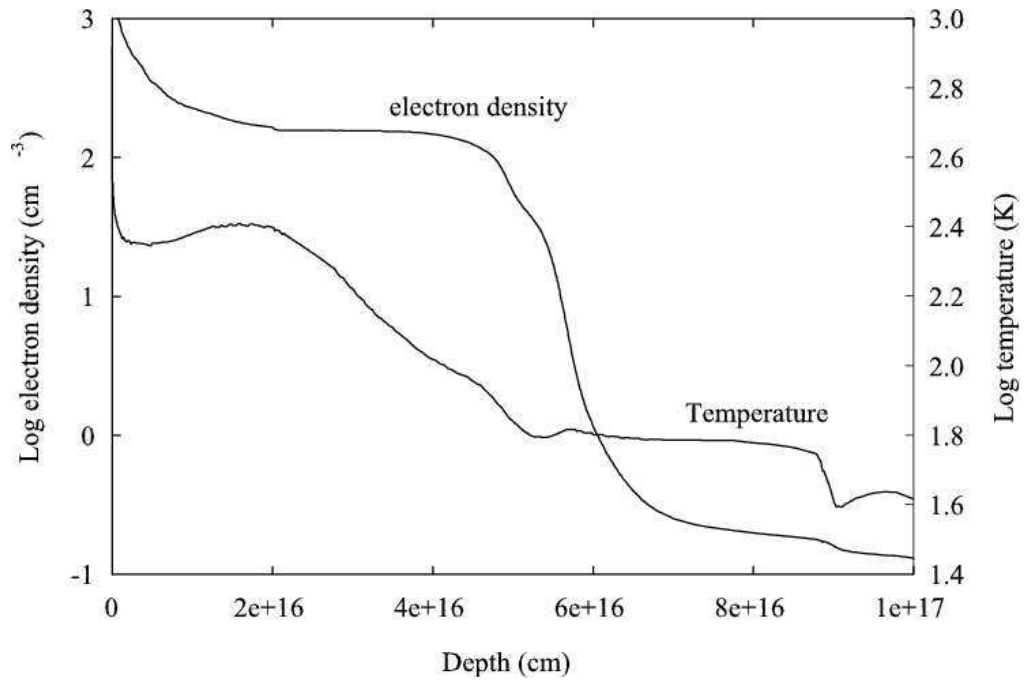


Figure 3. Figure 3, The predicted electron temperature and density structure. The total hydrogen density was assumed to be constant.